

Intragenic G-quadruplex structure formed in the human CD133 and its biological and translational relevance

Pasquale Zizza¹, Chiara Cingolani¹, Simona Artuso¹, Erica Salvati¹, Angela Rizzo¹, Carmen D'Angelo¹, Manuela Porru¹, Bruno Pagano², Jussara Amato², Antonio Randazzo², Ettore Novellino², Antonella Stoppacciaro³, Eric Gilson^{4,5}, Giorgio Stassi⁶, Carlo Leonetti^{1,*} and Annamaria Biroccio^{1,*}

¹Area of Translational Research, Regina Elena National Cancer Institute, via E. Chianesi 53, 00144 Rome, Italy,

²Department of Pharmacy, University of Naples 'Federico II', via D. Montesano 49, I-80131 Napoli, Italy, ³Dipartimento di Medicina Clinica e Molecolare, Università 'La Sapienza', piazzale Aldo Moro 5, 00185 Rome, Italy, ⁴Institute for Research on Cancer and Aging, Nice (IRCAN), CNRS UMR7284/INSERM U1081, University of Nice, 06107 Nice, France, ⁵Department of Medical Genetics, Archet 2 Hospital, CHU of Nice, 06202 Nice cedex 3, France and ⁶Department of Surgical and Oncological Sciences, University of Palermo, via del Vespro 131, 90127 Palermo, Italy

Received August 25, 2015; Revised October 13, 2015; Accepted October 14, 2015

ABSTRACT

Cancer stem cells (CSCs) have been identified in several solid malignancies and are now emerging as a plausible target for drug discovery. Beside the questionable existence of CSCs specific markers, the expression of CD133 was reported to be responsible for conferring CSC aggressiveness. Here, we identified two G-rich sequences localized within the introns 3 and 7 of the CD133 gene able to form G-quadruplex (G4) structures, bound and stabilized by small molecules. We further showed that treatment of patient-derived colon CSCs with G4-interacting agents triggers alternative splicing that dramatically impairs the expression of CD133. Interestingly, this is strongly associated with a loss of CSC properties, including self-renewing, motility, tumor initiation and metastases dissemination. Notably, the effects of G4 stabilization on some of these CSC properties are uncoupled from DNA damage response and are fully recapitulated by the selective interference of the CD133 expression.

In conclusion, we provided the first proof of the existence of G4 structures within the CD133 gene that can be pharmacologically targeted to impair CSC aggressiveness. This discloses a class of potential antitumoral agents capable of targeting the CSC subpopulation within the tumoral bulk.

INTRODUCTION

Colorectal cancer (CRC) is one of the main causes of tumor-related mortality worldwide. Although surgical resection represents the elective therapeutic approach for the treatment of the tumor at its early stage, more than 50% of patients develop a metastatic disease, which is incurable with the available therapies (1). Therefore, the development of innovative therapeutic strategies is of crucial importance. In the last few years, growing evidence supported the hypothesis of the existence, within primary tumors, of cell subpopulations, referred as cancer stem cells (CSCs), characterized by self-renewal capacity and resistance to 'conventional' anticancer therapies. Although CSCs represent a small fraction of the overall tumor, these cells possess the potential to initiate and sustain tumor growth and metastasis (2). Identification of CSCs is mainly based on the surface marker expression, including CD133, CD166 and CD44 (3,4). Interestingly, CD133 is associated with tumorigenicity and progression of the disease, since its up-regulation in CRC strongly correlates with poor prognosis and metastatic dissemination (5–7). CD44 is a membrane adhesion molecule that binds hyaluronic acid and contributes to cell–cell and cell–matrix adhesion, growth and tumor progression (8). Finally, CD166 belongs to the immunoglobulin superfamily of adhesion molecules involved in cell migration and growth (9), and its expression has been correlated with bad prognosis and shortened survival (10). Altogether, these studies strongly indicate that the cell-surface phenotype of CSC can be mechanistically linked with metastatic process, suggest-

*To whom correspondence should be addressed. Tel: +39 0652662569; Fax: +39 0652662592; Email: biroccio@ifo.it
Correspondence may also be addressed to Dr Carlo Leonetti. Tel: +39 0652662534; Fax: +39 0652662592; Email: leonetti@ifo.it

ing that the surface molecules could be clinically exploited both as a biomarker and therapeutic targets.

G-quadruplexes (G4s) are non-canonical DNA secondary structures widely described at the chromosome ends (11,12) and in the promoters of a wide range of genes important in cell signaling, recognized as hallmarks of cancer (13–16). Interest in the more general therapeutic significance of G4s is expanding to include G4 structures in 5'-UTR regions and introns. Indeed, G4 sequences localized in promoter region (within 1000 nt from the starting codon) or at the 5'-UTR, can affect the expression of the target gene by regulating the transcriptional or the translational processes, respectively (17,18). On the other hand, G4s formed in the introns (if localized nearby to the splice acceptor sites of the adjacent exons) can affect the activity of the splicing machinery causing intron retention events (19,20) that could be lastly responsible for the synthesis of immature RNA transcripts.

Over the past two decades, several G4-interacting small molecules, designed to act as G4 stabilizers, have been developed with the aim of identifying potential anticancer therapeutics (21,22). Notably, many G4s have physicochemical properties and structural characteristics that make them druggable, and their structural diversity suggests that a high degree of selectivity might be possible (23). More interestingly, G4 DNA structures have been detected in human cells, corroborating the application of stabilizing ligands as a new class of anticancer agents (24,25). In this area, our group and others have made important contributions in identifying new G4-stabilizing agents. The profiling of the biological properties of several G4-binders demonstrated that they are outstandingly potent in inducing selective DNA-damage at telomeres of cancer versus normal cells (21,26,27). In addition, these drugs can also affect the expression of a number of cancer related genes (15–17,28,29), showing a potent multimodal antitumoral activity, either alone or in combination with antineoplastic drugs (21,26,30–33).

Here, we provide evidence that G4 ligands can dramatically impair the tumor-promoting activity of colon CSCs through triggering an alternative splicing of the *CD133* mRNA, highlighting how G4 stabilization represents a valuable therapeutic option against CSCs.

MATERIALS AND METHODS

Cell culture, treatments and transfections

Patient derived colon CSC-enriched cell lines (CSC_1 and CSC_2) were obtained as previously described (34).

CSC-LUC, shCD133_1 and shCD133_2 cells were generated by transfecting the cells with the JetPEI® (Polyplus-transfection, Illkirch, France), according to the manufacturer's instructions. The following plasmids were used: PGL2 vector containing the firefly luciferase gene under the control of the SV promoter (Promega Madison, WI, USA), MISSION® *CD133* shRNAs TRCN0000424799 and TRCN0000416340 (Sigma-Aldrich, St. Louis, MO, USA).

Cells were grown in ultra-low attachment plates (Corning, Lowell, MA, USA) and maintained in stemness

medium (DMEM-F12, Euroclone, Milan, Italy) supplemented as reported in (34). When indicated, cells were plated under adherent condition in complete medium: DMEM (Euroclone) supplemented with 10% FCS (HyClone, Logan, UT, USA).

RHPS4, synthesized as already reported (35), was used at 1 μM concentration for different times. ATM-inhibitor KU-55933 (Sigma-Aldrich) was used at 5 μM for 96 h.

Immunofluorescence (IF)

For FACS analysis, untreated or treated cells were incubated with the following antibodies: anti human CD133 (mouse mAb AC133-Pur, Miltenyi Biotec, Bisley, UK), anti human CD44 (mouse mAb, BD Biosciences, San Diego, CA, USA) and anti human CD166 (mouse mAb, BD Biosciences); stained with FITC-conjugated Goat anti Mouse antibody (Jackson Immunoresearch, Suffolk, UK) and analyzed by flow cytometry using FACScalibur (BD Immunocytometry System-BDIS, San Jose, CA, US).

For microscopy analysis, untreated or treated cells were grown in complete medium and the IF analysis was performed (14), using the anti-CD133 antibody (AC133-PE, Miltenyi). Stained cells were analyzed with a Leica DMIRE2 microscope equipped with a Leica DFC 350FX camera and elaborated by a Leica FW4000 deconvolution software (Leica, Solms, Germany). For quantitative analysis of CD133 expression, 200 cells on triplicate slices were analyzed, and scored on the basis of the CD133 staining. In detail, the cells with isolated CD133 spots were considered CD133^{low}, while cells with a marked and continuous staining were considered CD133^{high}.

For interphase nuclei telomere-induced foci (TIFs) analysis, cells were fixed in 2% formaldehyde and permeabilized in 0.25% Triton X100 in phosphate buffered saline (PBS) for 5 min at room temperature (RT). For immunolabeling, cells were incubated with primary antibody (RT, 2 h), washed twice in PBS, and finally incubated with the secondary antibodies (RT, 1 h). The following primary antibodies were used: rabbit polyclonal anti-TRF1 antibody (Abcam Ltd., Cambridge, U.K.); mouse monoclonal anti-γH2AX antibody (Upstate, Lake Placid, NY, USA). The following secondary antibodies were used: TRITC-conjugated Goat anti Rabbit and FITC-conjugated Goat anti Mouse (Jackson Immunoresearch). Nuclei were counterstained with DAPI (Sigma-Aldrich).

Western Blotting

Western blot and detection were performed as previously reported (36). The activation state of DNA damage response proteins was analyzed by using the following antibodies: rabbit mAb anti-Ser1981 p-ATM (Abcam Ltd.); mouse mAb anti-p53 DO-1 and rabbit pAb anti-Thr68 p-CHK2 (Cell Signaling, Beverly, MA, USA). As loading control, levels of β-ACTIN were evaluated by using the mouse mAb anti-β-actin (Sigma-Aldrich).

RT-PCR

RNA, extracted with Trizol reagent (Invitrogen, Carlsbad, CA, USA), was converted to cDNA with the SuperScript

®VILO™ cDNA synthesis kit (Invitrogen). Evaluation of *CD133* expression and analysis of the splice variants were performed using the primers reported in Figure 3G. Densitometry was performed with ImageJ software version 1.40.

Polymerase stop assay

Polymerase Stop Assay was performed as already reported (14). Of note, the 77-mer DNA templates were generated starting from a scaffold sequence 5'-CTG GAG ATC CCC GCC GGG TAC CCG GGT GAG - insert -TAT AGT GAG TCG TAT TA-3', where the insert corresponds to the putative G4 sequences reported in Figure 2A.

Biophysical analyses

The sequences d(TGGGAAGGATGTGGGAGGAGAG GGCAGCGGGA) (intron 3(b)) and d(TGGGGATTGC CGGGCAGGGCTAACGCGTGGGT) (intron 7) were synthesized as already reported (37). Oligonucleotide samples were prepared by dissolving the lyophilized compound in potassium phosphate buffer (70 mM KCl, 10 mM KH₂PO₄, 0.2 mM EDTA, pH 7.0). The solutions were heated at 90°C for 5 min and slowly cooled to room temperature. The annealing procedure was followed by overnight storage at 4°C prior to use. The concentration of the oligonucleotides was evaluated by UV measurements at 260 nm, at a temperature of 90°C, using molar extinction coefficient values calculated by the nearest-neighbor model (38). Stock solutions of RHPS4 were prepared at 1–2 mM concentration in the same potassium phosphate buffer. Appropriate amounts of ligand were added to the oligonucleotide solutions to obtain the desired 2:1 and 4:1 ligand/DNA ratio, followed by mix at 25°C for 1 h, before data acquisition. CD spectra and melting experiments were recorded using a Jasco J-815 spectropolarimeter equipped with a thermoelectrically controlled cell holder (Jasco PTC-423S Peltier). A quartz cell of 1 mm optical path length was used. CD spectra at 25°C were the averages of three scans collected between 220 and 360 nm with a scanning rate of 100 nm/min, and a response time of 1 s. Buffer baseline was subtracted from each spectrum. CD melting were carried out in the 20–100°C temperature range, at 1°C/min heating rate by following changes of CD signal at the wavelengths of the maximum CD intensity. UV absorbance spectra were recorded using an Evolution 300 UV-Vis spectrophotometer (Thermo Scientific) equipped with a Peltier temperature controller. The 15 μM DNA solutions were placed in a quartz cuvette of 1 mm path length. Thermal difference spectra (TDS) were obtained by recording the absorbance spectra in the range 220–320 nm at 20 and 90°C and subsequently taking the difference between the two spectra (39).

Colony formation assay

Cells were grown in complete medium in absence or in presence of RHPS4 for different times. At the end of the treatment, 500 cells for each condition were seeded into 60-mm plates and after 10 days colonies were stained with 2% methylene blue in 95% ethanol and counted.

Sphere formation assay

Untreated or treated cells were grown for 96 h in stemness medium. At the end of the treatment, the primary tumorspheres were mechanically dissociated and the resulting cells were re-plated in stemness medium. After 5 days of growth, the secondary tumorspheres were analyzed and quantified by phase-contrast microscopy.

Cell migration

Chemotaxis was performed in a 48-wells Boyden chamber-slide using 8 μm pore-size polycarbonate filters (Neuro-Probe Inc, MD, US) (14). Briefly, the lower compartment of each well was filled with serum free medium with 0.1% BSA, as negative control, or 50 ng/ml SDF1α (Sigma-Aldrich). After 6 h, cells were fixed in EtOH 70% and stained using Crystal violet. Each point was run in triplicate. Cells on five random fields on the lower face of the filter were counted at 40X magnification.

In vivo experiments

Six to eight weeks old male mice CD-1 nude (nu/nu) and NOD.SCID (Harlan Laboratories, S. Pietro al Natisone, Italy) were used. All animal procedures were approved by the ethics committee of the Regina Elena National Cancer Institute (CE/534/12) and were in compliance with the national and international directives (D.L. March 4, 2014, no. 26; directive 2010/63/EU of the European Parliament and of the council; Guide for the Care and Use of Laboratory Animals, United States National Research Council, 2011).

CSC-LUC cells (10⁶ cells/mouse) pre-treated for 96 h with 1 μM RHPS4 or PBS (Vehicle) were intramuscularly injected into immunosuppressed CD-1 nu/nu mice (5 mice/group). Tumor appearance and growth were followed by caliper measurement and bioluminescence imaging analysis. CSC-LUC cells (6 mice/group) treated as before, were also injected in the spleen of anesthetized NOD.SCID mice and after 30 min the spleen was removed. Seven days post-injection, the mice were sacrificed, liver and gastrointestinal organs harvested and imaged. Real time tumor dissemination in the whole mice and in organs was imaged using the IVIS imaging system 200 series (Caliper Life Sciences, Hopkinton, MA, USA). Data were acquired and analyzed using the living image software version 3.0 (Caliper Life Sciences).

Statistical analysis

The Student's *t*-test (unpaired, two-tailed) was used for comparing statistical differences. Survival curves of mice were generated by Kaplan–Maier product-limit estimate, and statistical differences between the various groups were evaluated by log-rank analysis with Yates correction (software Primer of Biostatistics, McGraw-Hill, New York, NY, USA). Differences were considered statistically significant when *P* < 0.05.

RESULTS

G4 ligands can inhibit CD133 expression in colon CSCs

CSCs have been recently recognized as the main cause of treatment failure in several human malignancies (40). In

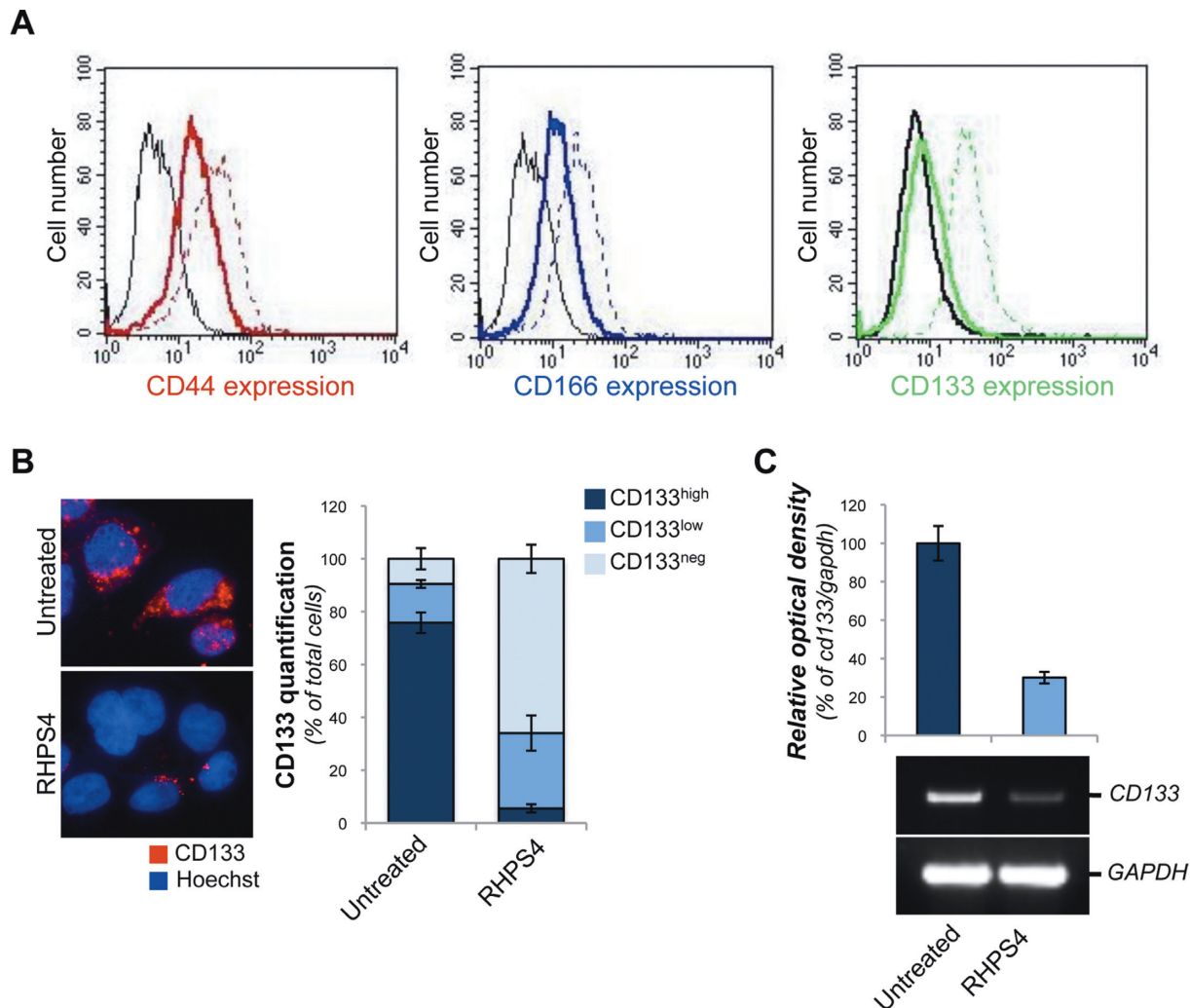


Figure 1. Expression of CD133 is impaired by G4 ligand treatment. (A) Colon CSCs (CSC_1), untreated or treated with 1 μ M RHPS4 for 96 h, were immunostained with the antibodies against CD44, CD166 or CD133 and processed for FACS analysis. Histograms represent the fluorescence intensities in the negative controls (black lines), untreated (colored dashed lines) and treated (colored solid lines) samples. (B) CSC_1 cells were treated as in A and the expression of CD133 was analyzed by IF microscopy. Left panel: representative Immunofluorescence (IF) pictures are shown (63X magnification). Right panel: quantification of IF reporting the percentage of cells not expressing (CD133^{neg}) or expressing high (CD133^{high}) and low (CD133^{low}) CD133 levels. (C) RT-PCR analysis of *CD133* gene. The histogram shows the relative optical density of *CD133*. A representative picture of PCR products is shown. Histograms show the mean values \pm SD of at least three independent experiments.

spite of the continuous efforts in developing new molecules able to target CSCs, identification of really efficacious drugs has not been reported so far. Here, based on data describing G4 ligands as a new promising class of anticancer agents (28,41), we evaluated the effects of these molecules on patient-derived colon CSCs.

First, the typical properties of CSCs, including the expression of surface markers (CD44, CD166 and CD133), resistance to Oxaliplatin and 5-Fluorouracil, the two drugs routinely used in treatment of colorectal cancers, and the tumor-initiating potential were evaluated in two patient-derived colon CSCs (CSC_1 and CSC_2), and in two stabilized colon cancer cell lines (HCT116 and HT29) used as control (Supplementary Figure S1A–C). Interestingly, immunohistochemistry analyses revealed that the tumors originating from the CSCs are endowed with the ability to self-renew and faithfully reproduce the original tumor in im-

munocompromised mice, recapitulating some key points to be considered for the translatability of experimental findings (Supplementary Figure S1D).

Then, we investigated the ability of G4 ligands (Supplementary Figure S2) to affect CSC marker expression. Strikingly, despite a slight reduction of CD44 and CD166 levels, RHPS4, an effective and well-characterized G4 ligand (26,33,35,42–45), almost completely impaired the expression of CD133 (Figure 1A and Supplementary Figure S3A), and this potent inhibitory effect was also observed with two novel RHPS4-derivative molecules (Supplementary Figures S4A and S4B), characterized by improved on- and off-target profile (46,47), and, even if at a different extent, with Emicorone (Supplementary Figure S4C), a chemically unrelated G4 ligand, showing high selectivity for quadruplex versus duplex DNA and triggering telomere damage and antitumoral activity in mice (48,49).

A

TARGET	SEQUENCE	START	STOP	LENGTH	SCORE
CD133 Promoter	<u>GGGC</u> <u>GGG</u> GAGCAGGAGC <u>GGG</u> GCC <u>GGG</u>	-221	-196	26	37
CD133 intron 2	<u>GGG</u> CAGAGCC <u>GGT</u> <u>GGG</u> <u>AT</u> <u>GGG</u> T <u>GGG</u>	+37815	+37839	25	33
CD133 intron 3 (a)	<u>GGGG</u> <u>AT</u> <u>GGG</u> T <u>GG</u> <u>AGGG</u> T <u>CA</u> <u>GT</u> <u>AGGG</u>	+48327	+48353	27	38
CD133 intron 3 (b)	<u>GGGA</u> <u>AGG</u> <u>AT</u> <u>GT</u> <u>GGG</u> <u>AGG</u> <u>AGGG</u> <u>CAGC</u> <u>GGG</u>	+50445	+50474	30	38
CD133 intron 7	<u>GGGG</u> <u>ATT</u> <u>GCC</u> <u>GGG</u> <u>CAGG</u> <u>GCTA</u> <u>AGCG</u> <u>GGG</u>	+57626	+57654	29	36
Telomere	(<u>GGG</u> <u>TTA</u> <u>GGG</u> <u>TTA</u> <u>GGG</u> <u>TTA</u> <u>GGG</u>) _n	-	-	-	42

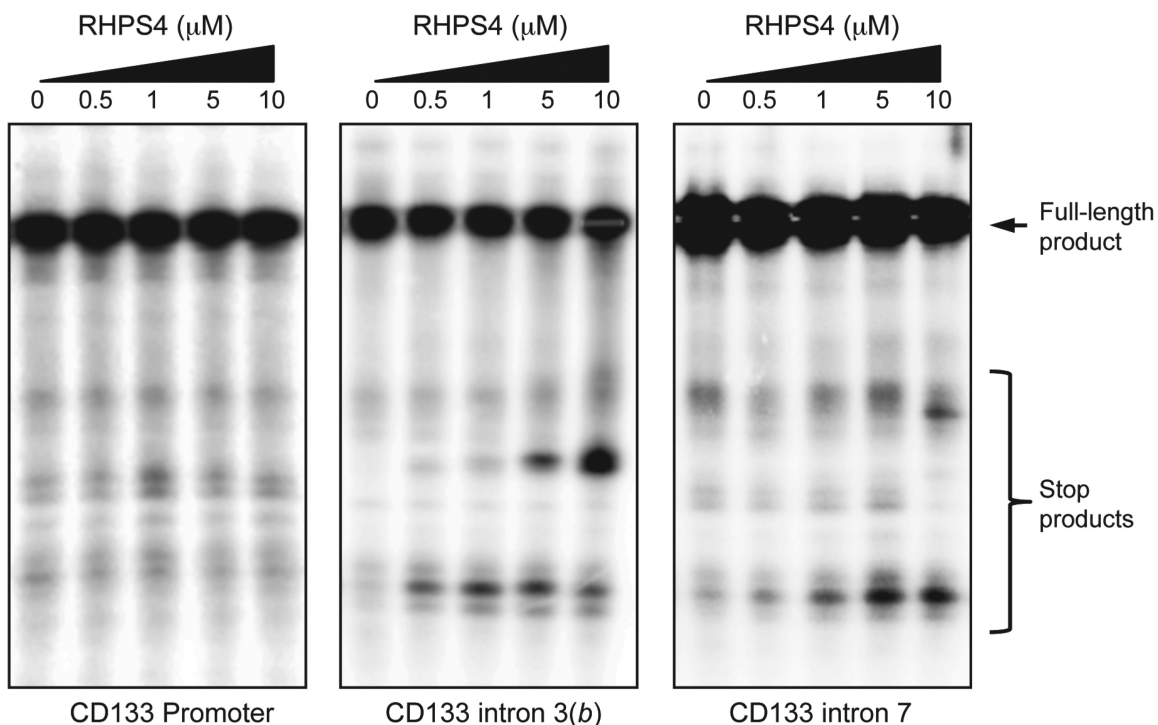
B

Figure 2. *CD133* gene contains several putative G4-forming sequences. (A) The table shows the putative G4s identified within the *CD133* gene. For each sequence is reported the score, calculated by QGRS mapper (G4 structure prediction software www.bioinformatics.ramapo.edu/QGRS/analyze.php). For comparison, the score of the human telomere repeat is reported. (B) Polymerase stop assay. Oligonucleotides reproducing the G4 sequences identified in the promoter and within the introns 3 and 7 of *CD133* were amplified by PCR in presence of 5 mM KCl plus increasing concentrations of RHPS4. The stop products indicate the presence of stabilized G4 structures. Data shown are representative of three independent experiments.

Moreover, a single-cell morphological analysis performed by IF microscopy (Figure 1B and Supplementary Figure S3B) revealed that, treatment with RHPS4 induced a robust decrease in the amount of *CD133*^{high} cells with a concomitant increases in both *CD133*^{low} and *CD133*^{neg} cell subpopulations. Finally, to assess whether RHPS4 exerts its inhibitory effect by acting at transcriptional level, expression of the *CD133* gene was evaluated. RT-PCR showed that treatment with the G4 ligand decreases the level of *CD133* (Figure 1C and Supplementary Figure S3C), without substantially affecting the *CD44* and *CD166* mRNAs (Supplementary Figure S3D), suggesting the presence of

at least one RHPS4-sensitive G-rich sequence within the *CD133* gene.

Down-regulation of *CD133* expression is dependent on the stabilization of intragenic G4 sequences

Following the initial identification of *CD133* as RHPS4-sensitive CSC target, we investigated the mechanism(s) through which this G4 ligand regulates its expression. G4 structures are not exclusively located at the chromosome ends; indeed, these structures have been recently found along the entire genome (and on certain RNA transcripts) and their functions can range from transcriptional control to splicing regulation (20,41,50). Based on these data, we

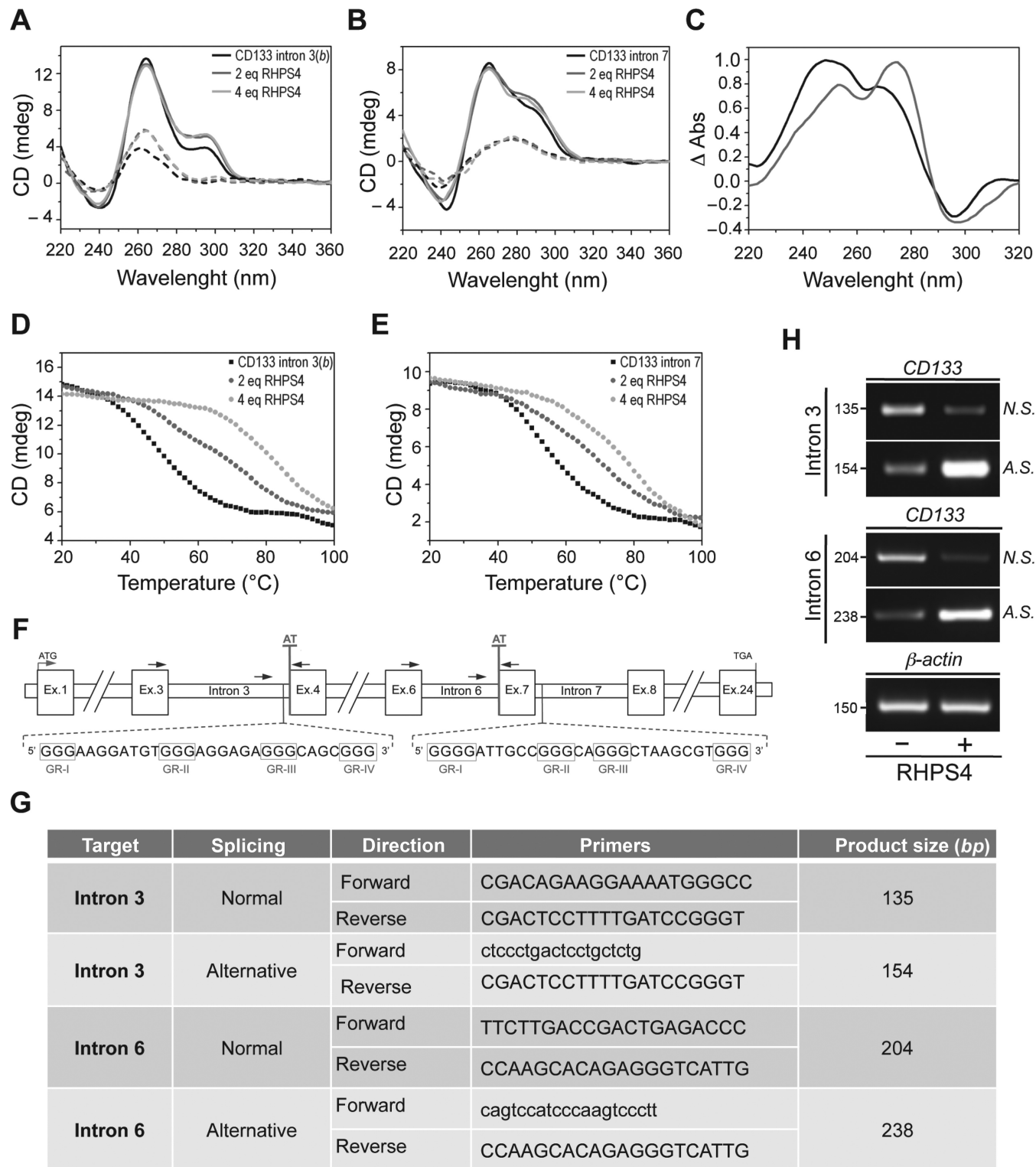


Figure 3. Stabilization of *CD133* intragenic G4 sequences determines alternative splicing events. (A and B) CD spectra of the G4-forming DNA sequences found in the *CD133* introns 3 and 7 at 20°C (black solid lines), 90°C (black dashed lines), and in presence of the indicated doses of RHPS4 at 20°C (gray solid lines) and 90°C (gray dashed lines). (C) Normalized thermal difference spectra of intron 3(b) (black solid line) and 7 G4s (gray solid line). (D and E) CD melting profiles of intron 3(b) and 7 G4-forming sequences in the absence (filled squares) and in the presence of the indicated doses of RHPS4 ligand (gray circles). (F) Scheme showing the positioning of the G4s within the introns 3 and 7 of *CD133*. For each sequence is indicated the proximal exon acceptor splicing site (AT). The arrows indicate the positioning and orientation of the primers designed for evaluating the splicing. (G) Nucleotide sequences of the primer used to discriminate between the normal and the alternative splicing of intron 3 and 6 of *CD133*. For each pair of primers, the size of the amplification product is indicated. (H) RT-PCR analysis of alternative splicing in CSC_1 cells untreated or treated with RHPS4 (1 μ M for 96 h). Normal (N. S.) and alternative (A. S.) splicing of intron 3 and 6 were evaluated. Expression levels of β -ACTIN were measured as loading control.

performed an *in silico* analysis on the entire *CD133* gene looking for putative G4 sequences. Interestingly, the broad analysis carried by QGRS G4 structure prediction software (51) revealed the presence of five G-rich strands (one located within the promoter region and the other four within the introns 2, 3 and 7), whose probability to arrange into stable G4 structures (G-score) was very similar to that of the human telomeric repeats (TTAGGG)_n (Figure 2A). The existence of these structures might explain the inhibitory effect of RHPS4 on the expression of *CD133*.

Although all the identified target sequences had almost the same probability to form G4 structures, the G-rich motif located within the intron 2 and the first of the two identified in the intron 3(a), based on their huge distance from the proximal exon acceptor splicing sites (>1000 bp), were excluded from any additional investigation. The sequences found within the promoter and those found in the intron 3(b) and intron 7, were assayed for their capability to fold into stable G4 structures *in vitro*. First, we performed a polymerase stop assay (14,52) to exploit the capability of stable secondary DNA structures of arresting the activity of the DNA polymerase, allowing us to recognize those G-rich sequences that, under adequate conditions, fold into stable G4s. As showed in the Figure 2B, increasing concentrations of RHPS4 lead to a dose-dependent accumulation of stop products corresponding to the G-strands of the introns 3(b) and 7, whilst no effects were observed with the promoter candidate sequence.

Then, the two target sequences of the introns 3(b) and 7 were investigated by circular dichroism (CD) in order to determine the folding topology of G4s in solution (53), as well as to evaluate the ability of a G4 ligand to stabilize or alter these structures (54). Interestingly, the CD spectra indicated that the two oligonucleotides actually folded into G4 structures in the presence of K⁺ (Figure 3A and B), despite the presence of extended loops that could, in principle, compromise the stability of a G4 (55,56). Specifically, the spectrum of the intron 3(b) G-rich sequence was characterized by a negative band at about 240 nm and an intense positive band at 264 nm, typical of parallel-stranded G4s. While the spectrum of the sequence identified within the intron 7 showed a negative band at about 240 nm and a positive band at 265 with a shoulder at 288 nm, consistent with the presence of a hybrid G4 structure. Then, the formation of G4 motifs was confirmed by UV TDS analysis (Figure 3C), showing the characteristic G4 signature (39), i.e. the negative band at 295 nm and the positive ones at around 270 and 250 nm. The stability of these G4s was evaluated by CD melting experiments. In both cases, the melting experiments showed a sigmoidal transition curve (Figure 3D and E) from which the melting temperatures (T_m) were found to be 48.2 (± 0.5) and 55.3 (± 0.5)°C for intron 3(b) and 7 G4s, respectively. CD spectra and melting experiments were also performed to analyze the effect of RHPS4 on the structure and stability of G4s in solution. As shown in Figure 3A and B, no significant variations of CD spectra were observed for the investigated G4s upon RHPS4 addition (up to 4 equivalents), suggesting that the overall structure is preserved. On the other hand, increasing concentrations of RHPS4 induced a significant dose-dependent increase of thermal stability of the structures, indicating a tight interaction with

the G4-forming sequences. Indeed, the CD melting curves (Figure 3D and E) showed that RHPS4 increased the T_m of 3(b) G4 of about 17 and 34°C at a 2:1 and 4:1 ligand/DNA ratio, respectively. While the ligand-induced increase in the T_m of the intron 7 G4 was of about 12 and 23°C at 2:1 and 4:1 ratio, respectively.

Finally, we investigated whether the formation of G4 structures within the introns 3 and 7 may affect the splicing of *CD133*. Since the two G4s are located 118 bp upstream and 261 bp downstream of the acceptor sites of the exons 4 and 7, respectively (Figure 3F), we evaluated, using appropriately designed primers (Figure 3G), the effect of the G4 stabilization on the splicing of intron 3 and 6. We found that the RHPS4 treatment leads to a marked reduction of the mature transcripts counterbalanced by an increase in the splicing variants corresponding to an inhibition of the intron excision (Figure 3H). Overall these data indicate that the formation of stable intronic G4s could affect the proper positioning of the splicing machinery consequently interfering with the process of RNA maturation. Indeed, the inclusion of each of the two introns (3 and 6) leads to the formation of premature stop codons that can explain the reduction of *CD133* expression.

G4 ligands can impair the tumorigenic potential of colon CSCs

The above results raise the interesting possibility that pharmacological G4 stabilization may affect the CSC activity. To address this question, the capability of RHPS4 to modulate the stemness properties of colon CSCs was assessed both *in vitro* and *in vivo*. Of note, these assays were performed by treating the cells for 96 h with 1 μ M of RHPS4, an experimental setting that reduces the expression of *CD133* without any overt effect on cell viability or apoptosis (Supplementary Figure S5A–C). Interestingly, both colony and sphere formation assay revealed that G4 ligands reduced cell survival up to about 50% (Figure 4A and B and Supplementary Figure S4D and E). Indeed G4 ligand treatments not only impaired self-renewal capability of the cells (Figure 4B, left panel and Supplementary Figure S4E, left panel) but, as revealed by qualitative microscopy analysis (Figure 4B, right panel and Supplementary Figure S4E, right panel), also significantly reduced the size of the spheres. Then, cell migration, evaluated in presence of SDF1 α , a potent chemoattractant cytokine, was almost completely abolished in RHPS4 pre-treated cells (Figure 4C). This effect was fully recapitulated by interference experiments performed by using two different short hairpin RNAs selective for *CD133* (sh*CD133_1* and sh*CD133_2*) (Figure 4C and D). Moreover, since RHPS4 is a potent inducer of DNA damage, including at the telomeres (Supplementary Figure S5D and E), the effect of RHPS4 was assessed also in presence of KU-55933, a specific ATM inhibitor (57). Notably, pharmacological inhibition of DDR pathway (Supplementary Figure S5D) did affect neither the expression of *CD133* (Supplementary Figure S5F) or the cell migration (Figure 4C), indicating that impairment of certain stemness properties by G4 ligands can be independent from the activation of the DNA damage response.

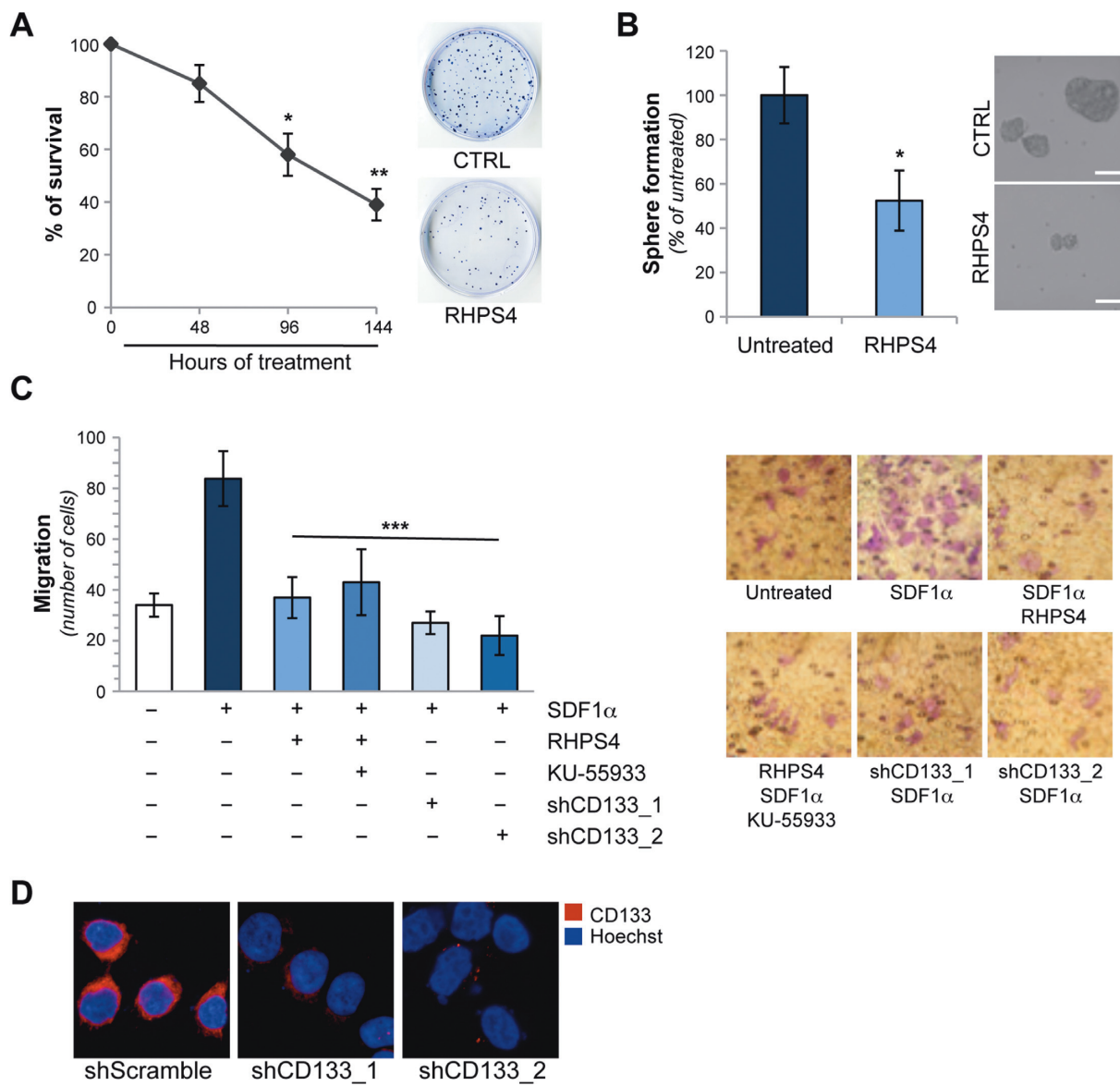


Figure 4. G4 stabilization impairs CSCs features *in vitro*. (A) Colon CSCs (CSC_1) were treated with 1 μ M of RHPS4 for the indicated times and colony forming ability was evaluated. The graph shows the surviving fractions calculated as the ratio of absolute survival of the treated sample/absolute survival of the control sample. Representative images of colony assay for untreated and 96 h treated sample are shown. (B) Primary tumorspheres, untreated or treated with RHPS4 (1 μ M for 96 h), were dissociated and the cell ability of originating secondary spheres was evaluated. The histogram shows the percentage of secondary tumorspheres obtained 5 days after dissociation. Representative images of secondary tumorspheres are shown in the right panel. (C) CSC_1 cells, treated as reported (RHPS4 1 μ M for 96 h, KU-55933 5 μ M for 96 h), or interfered for 48 h with two different shRNA constructs targeting CD133 (shCD133_1 and shCD133_2), were processed for chemotaxis assay in response to SDF1 α (50 ng/ml). Histograms represent the number of migrating cells. For each condition, representative pictures of cell migration (40X magnification) are reported. (D) Analysis of CD133 expression in colon CSC_1 cells 48 h after the transfection with a control shRNA (shScramble) and two different shRNA constructs targeting CD133. Representative IF images are shown. Graphs show the mean \pm SD of three independent experiments (* $P < 0.1$; ** $P < 0.01$; *** $P < 0.001$).

Finally, the effects of RHPS4 on the tumorigenic potential of CSCs were assessed *in vivo*. Pre-treatment with RHPS4 markedly impaired the aggressiveness of colon CSCs in immunosuppressed mice (Figure 5). Indeed, bioluminescence analysis performed at day 25 after cell injection showed that while in control group all the mice (5/5) developed tumors, in the RHPS4 group only one out of the five (1/5) injected mice developed tumor (Figure 5A). Afterwards, the tumor mass was detectable in the rest of mice (Figure 5B) but with a median time of tumor ap-

pearance of 29 days significantly reduced ($P < 0.01$) compared to that observed in untreated group (16 days). The delay in tumor development resulted in a different tumor growth rate as at day 67 the tumor weight in RHPS4-treated group was significantly decreased (660 ± 320) compared to untreated group (1747 ± 682 , $P = 0.012$). Moreover, being the high metastatic potential one the main features of CSCs, we evaluated the efficacy of RHPS4 on an experimental model of disseminated disease established after intrasplenic injection of colon CSCs, stably transfected

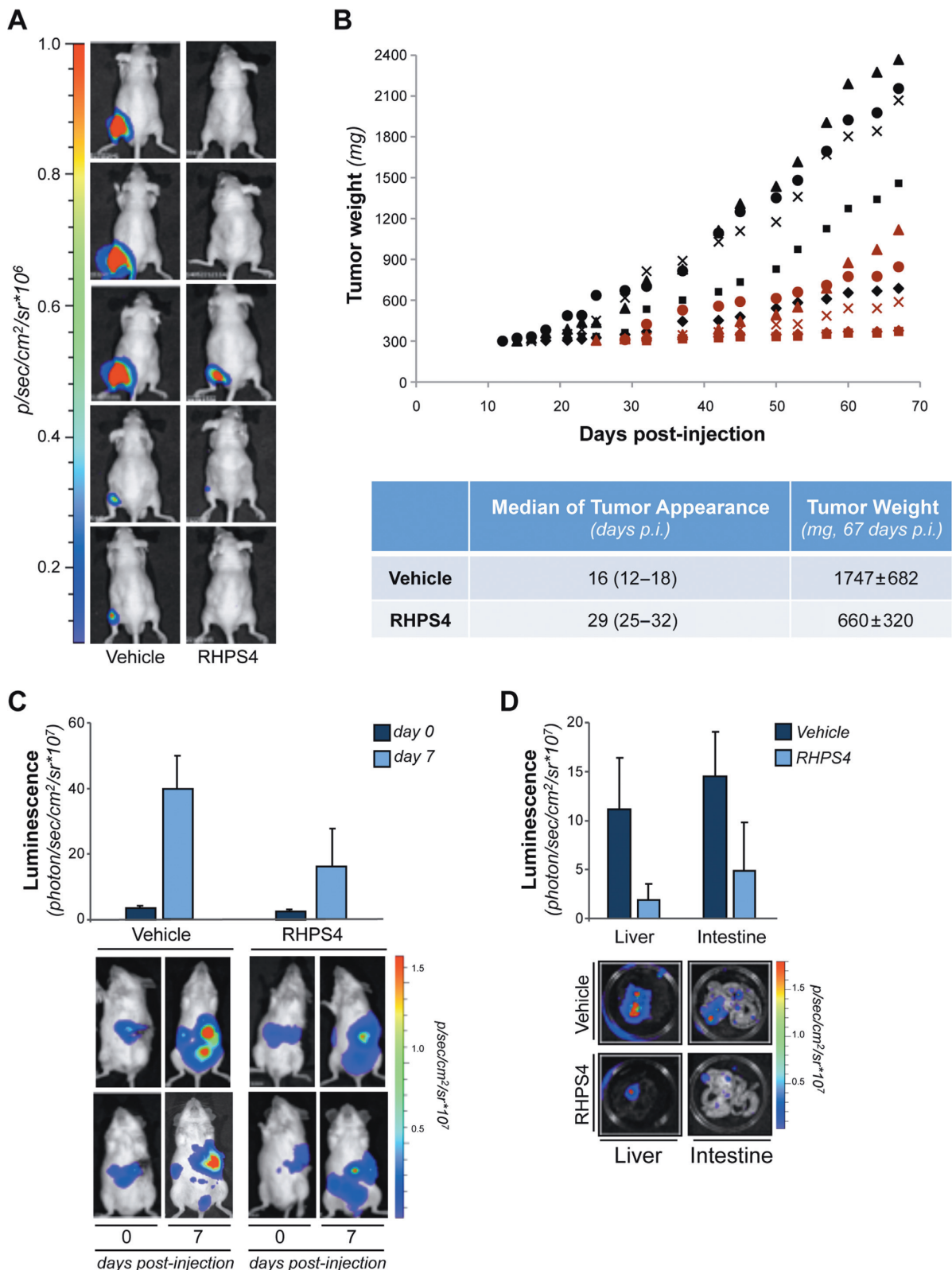


Figure 5. G4 stabilization impairs CSCs tumor promoting activity *in vivo*. (A and B) CSC-LUC cells, pre-treated for 96 h with 1 μ M of RHPS4 or a vehicle, were intramuscularly injected in immunosuppressed mice. (A) Luminescence images (quantified as number of photons/s) acquired 25 days after cell injection are shown. (B) Tumor weights assessed in mice intramuscularly injected with CSC-LUC cells treated with RHPS4 (red symbols) or Vehicle (black symbol) are reported. Each symbol represents a different mouse. Median of tumor appearance and average tumor weight are reported in the table. (C and D) CSC-LUC cells treated as in A were injected in the spleen of NOD-SCID mice and the real time tumor dissemination was monitored by the imaging system. (C) Histograms report bioluminescence in the whole mice at time 0 (immediately after the spleen removal) and at day 7 after tumor cells injection. Representative images of 2/6 mice/group are shown. (D) At day 7, mice were sacrificed and organs were harvested and analyzed. Histograms report bioluminescence in liver and gastrointestinal organs. Representative images of liver and intestine are also shown. Bars indicate mean values \pm SD.

with a luciferase-expressing vector. Interestingly, RHPS4 pre-treatment limited the colon CSCs dissemination being the luminescence of treated animals significantly reduced (about 50%) in comparison to that of the untreated ones. This is evident in the analysis performed both on the whole mice (Figure 5C, $P = 0.023$) and on the organs (liver $P = 0.026$ and intestine, $P = 0.038$) excised after the euthanization of animals (Figure 5D).

DISCUSSION

Over the last decade, CSC biology has acquired a huge relevance both at basic and preclinical cancer research level. In this context, particular attention has been paid to the biological relevance of stemness markers. The significance of these surface proteins expression, initially considered as CSCs specific markers, has been extensively debated in the last few years (58). Indeed, a number of recent studies reported that these proteins would be detectable, even if at lower levels, also in more differentiated cell types, questioning their real CSCs specificity (59). However, beside this controversial issue, the expression of these surface proteins was reported to be responsible for conferring CSC peculiar properties, including chemoresistance, self-renewal capability and metastatic potential (60,61). Here, we found that G4 ligands, including the well-characterized RHPS4, two novel RHPS4-derivatives, and Emicorin, markedly affect the stemness properties of patient-derived colon CSCs by impairing the expression of CD133. Although the effect of RHPS4 in counteracting the growth of CSCs was already proposed by Burger *et al.* in 2007, the mechanism through which the drug acts was not deeply investigated (43).

G4 structures, first identified at the chromosome ends, were found dislocated along the entire genome (and in the RNAs) (41,62–64) and their stabilization has been demonstrated to affect, through modulation of transcription (50), translation (65) or splicing (20), the expression of various target genes (15,16,66). Based on these data, and with the intent of defining the mechanism through which the G4 ligands can affect the expression of CD133, we analyzed the entire gene sequence, looking for G-rich strands with features compatible with the formation of G4 structures. Among the putative G4 sequences identified by bioinformatic analysis, two motifs (located within introns 3 and 7, respectively) were experimentally validated by CD. Notably, the CD analysis evidenced that both G4s are stabilized by RHPS4, affecting the process of transcript maturation, which, in turn, generated two alternatively spliced mRNAs, each deriving from a distinct event of intron retention. To date a number of *CD133* splice variants have been reported (67). However, the two splice variants induced by treatment with G4 ligand were never described, suggesting that these transcripts could generate aberrant CD133 isoforms that are then degraded. In line with these data, we found that intron retention determined the formation of premature stop codons leading to the production of truncated forms, probably removed by the nonsense-mediated decay pathway. In several cases, CD133 isoforms, derived from alternative splicing events, were not recognized by specific antibodies due to the lack of the AC133 epitope (68). At this level, we cannot completely exclude that the reduc-

tion observed in the CD133 protein expression could be due to the loss of the immunogenic epitope. However, data in the literature clearly indicate that AC133 epitope is, *per se*, sufficient to confer the aggressive phenotype to CSCs (68). Therefore, independently on the mechanism, our *in vitro* and *in vivo* functional studies clearly demonstrate that treatment of colon CSCs with the G4 ligand determines an almost complete impairment of their tumor-promoting activity both in terms of self-renewal and metastatic potential. Of note, other relevant stemness marker of colon CSCs (i.e. CD44 and CD166) were found slightly reduced by the drug treatment. Even though a cross-talk among different stemness markers has been described (4), we cannot completely exclude that G4 ligand might directly affect their expression by stabilizing G4 structures within their promoters as revealed by the QGRS G4 structure prediction software (51). Therefore, even if other genes can contribute to the biological effects observed with the G4 ligand on colon CSCs, the possibility of fully recapitulating the effects of the drug by specific interfering RNAs, indicates that treatment with G4 stabilizing agents inhibits the tumor-promoting signaling pathways regulated by CD133 (69,70).

CSCs for their aggressiveness and resistance to canonical therapeutics have been recognized as the main cause of failure in the treatment of several malignancies. Therefore, identification of a new class of antineoplastic drugs able to target these cells is of crucial importance. Here, we provide, for the first time, the evidence for the existence of intragenic G4 structure formed in the human *CD133*, corroborating the application of stabilizing ligands in a cellular context to target G4 and interfere with gene expression and function. Indeed, these molecules, initially designed to bind to and stabilize the telomeric G4 sequences, triggering telomere damage and cell death, can act, through a multimodal therapeutic strategy, on the expression of cancer-related genes, including the *CD133*, counteracting the tumor-promoting activity of colon CSCs. Notably, being *CD133* relevant in the progression of tumors of different histotype, it will be possible to extend our results also to other malignancies. Moreover, since the folding of G4s localized within the genes can assume different shapes, depending on their specific DNA sequence, it might be possible to design and develop new and more potent drugs able to selectively hit certain, well-defined, drivers depending on the tumor histotype.

In conclusion, here, we provided an additional proof of the potential therapeutic use of G4 ligands as a novel multi-targeting anticancer strategy. Moreover, the ability of these drugs to directly target CSCs derived from patients and the use of advanced preclinical colorectal cancer models, significantly increases the possibility to translate our results in clinical studies.

SUPPLEMENTARY DATA

Supplementary Data are available at NAR Online.

ACKNOWLEDGEMENT

The authors thank Prof. Ruggero De Maria for the critical reading of the manuscript and Prof. Armandodoriani

Bianco for Emicorin synthesis. C.C. is recipient of a fellowship from the Italian Foundation for Cancer Research (FIRC).

FUNDING

Italian Association for Cancer Research [#11567, #9979 to A.B, #14337 to C.L. and #14150 to A.R.]. Funding for open access charge: Italian Association for Cancer Research [#11567, #9979 to A.B, #14337 to C.L. and #14150 to A.R.].

Conflict of interest statement. None declared.

REFERENCES

- Guglielmi,A., Ruzzene,A., Conci,S., Valdegamberi,A., Vitali,M., Bertuzzo,F., De Angelis,M., Mantovani,G. and Iacono,C. (2014) Hepatocellular carcinoma: surgical perspectives beyond the barcelona clinic liver cancer recommendations. *World J. Gastroenterol.*, **20**, 7525–7533.
- Zeuner,A., Todaro,M., Stassi,G. and De Maria,R. (2014) Colorectal cancer stem cells: from the crypt to the clinic. *Cell Stem Cell*, **15**, 692–705.
- Klonisch,T., Wiechec,E., Hombach-Klonisch,S., Ande,S.R., Wesselborg,S., Schulze-Osthoff,K. and Los,M. (2008) Cancer stem cell markers in common cancers - therapeutic implications. *Trends Mol. Med.*, **14**, 450–460.
- Horst,D., Kriegl,L., Engel,J., Kirchner,T. and Jung,A. (2009) Prognostic significance of the cancer stem cell markers CD133, CD44, and CD166 in colorectal cancer. *Cancer Invest.*, **27**, 844–850.
- Ricci-Vitiani,L., Lombardi,D.G., Pilozzi,E., Biffoni,M., Todaro,M., Peschle,C. and De Maria,R. (2007) Identification and expansion of human colon-cancer-initiating cells. *Nature*, **445**, 111–115.
- Catalano,V., Di Franco,S., Iovino,F., Dieli,F., Stassi,G. and Todaro,M. (2012) CD133 as a target for colon cancer. *Expert Opin. Ther. Targets*, **16**, 259–267.
- Kashihara,H., Shimada,M., Kurita,N., Iwata,T., Sato,H., Kozo,Y., Higashijima,J., Chikakiyo,M., Nishi,M. and Matsumoto,N. (2014) CD133 expression is correlated with poor prognosis in colorectal cancer. *Hepatogastroenterology*, **61**, 1563–1567.
- Todaro,M., Francipane,M.G., Medema,J.P. and Stassi,G. (2010) Colon cancer stem cells: promise of targeted therapy. *Gastroenterology*, **138**, 2151–2162.
- Swart,G.W. (2002) Activated leukocyte cell adhesion molecule (CD166/ALCAM): developmental and mechanistic aspects of cell clustering and cell migration. *Eur. J. Cell Biol.*, **81**, 313–321.
- Weichert,W., Knosel,T., Bellach,J., Dietel,M. and Kristiansen,G. (2004) ALCAM/CD166 is overexpressed in colorectal carcinoma and correlates with shortened patient survival. *J. Clin. Pathol.*, **57**, 1160–1164.
- Han,H. and Hurley,L.H. (2000) G-quadruplex DNA: a potential target for anti-cancer drug design. *Trends Pharmacol. Sci.*, **21**, 136–142.
- Kelland,L. (2007) Targeting the limitless replicative potential of cancer: the telomerase/telomere pathway. *Clin. Cancer Res.*, **13**, 4960–4963.
- Balasubramanian,S., Hurley,L.H. and Neidle,S. (2011) Targeting G-quadruplexes in gene promoters: a novel anticancer strategy? *Nat. Rev. Drug Discov.*, **10**, 261–275.
- Salvati,E., Zizza,P., Rizzo,A., Iachettini,S., Cingolani,C., D'Angelo,C., Porru,M., Randazzo,A., Pagano,B., Novellino,E. et al. (2014) Evidence for G-quadruplex in the promoter of vegfr-2 and its targeting to inhibit tumor angiogenesis. *Nucleic Acids Res.*, **42**, 2945–2957.
- Siddiqui-Jain,A., Grand,C.L., Bearss,D.J. and Hurley,L.H. (2002) Direct evidence for a G-quadruplex in a promoter region and its targeting with a small molecule to repress c-MYC transcription. *Proc. Natl. Acad. Sci. U.S.A.*, **99**, 11593–11598.
- Rodriguez,R., Miller,K.M., Forment,J.V., Bradshaw,C.R., Nikan,M., Britton,S., Oelschlaegel,T., Xhemalce,B., Balasubramanian,S. and Jackson,S.P. (2012) Small-molecule-induced DNA damage identifies alternative DNA structures in human genes. *Nat. Chem. Biol.*, **8**, 301–310.
- Brown,R.V. and Hurley,L.H. (2011) DNA acting like RNA. *Biochem. Soc. Trans.*, **39**, 635–640.
- Bugaut,A. and Balasubramanian,S. (2012) 5'-UTR RNA G-quadruplexes: translation regulation and targeting. *Nucleic Acids Res.*, **40**, 4727–4741.
- Didiot,M.C., Tian,Z., Schaeffer,C., Subramanian,M., Mandel,J.L. and Moine,H. (2008) The G-quartet containing FMRP binding site in FMR1 mRNA is a potent exonic splicing enhancer. *Nucleic Acids Res.*, **36**, 4902–4912.
- Marcel,V., Tran,P.L., Sagne,C., Martel-Planche,G., Vaslin,L., Teulade-Fichou,M.P., Hall,J., Mergny,J.L., Hainaut,P. and Van Dyck,E. (2011) G-quadruplex structures in TP53 intron 3: role in alternative splicing and in production of p53 mRNA isoforms. *Carcinogenesis*, **32**, 271–278.
- Neidle,S. (2010) Human telomeric G-quadruplex: the current status of telomeric G-quadruplexes as therapeutic targets in human cancer. *FEBS J.*, **277**, 1118–1125.
- Muller,S. and Rodriguez,R. (2014) G-quadruplex interacting small molecules and drugs: from bench toward bedside. *Expert Rev. Clin. Pharmacol.*, **7**, 663–679.
- Zhang,S., Wu,Y. and Zhang,W. (2014) G-quadruplex structures and their interaction diversity with ligands. *ChemMedChem*, **9**, 899–911.
- Biffi,G., Tannahill,D., McCafferty,J. and Balasubramanian,S. (2013) Quantitative visualization of DNA G-quadruplex structures in human cells. *Nat. Chem.*, **5**, 182–186.
- Henderson,A., Wu,Y., Huang,Y.C., Chavez,E.A., Platt,J., Johnson,F.B., Brosh,R.M. Jr, Sen,D. and Lansdorp,P.M. (2014) Detection of G-quadruplex DNA in mammalian cells. *Nucleic Acids Res.*, **42**, 860–869.
- Salvati,E., Leonetti,C., Rizzo,A., Scarsella,M., Mottolese,M., Galati,R., Sperduti,I., Stevens,M.F., D'Incalci,M., Blasco,M. et al. (2007) Telomere damage induced by the G-quadruplex ligand RHPS4 has an antitumor effect. *J. Clin. Invest.*, **117**, 3236–3247.
- Salvati,E., Rizzo,A., Iachettini,S., Zizza,P., Cingolani,C., D'Angelo,C., Porru,M., Mondello,C., Aiello,A., Farsetti,A. et al. (2015) A basal level of DNA damage and telomere deprotection increases the sensitivity of cancer cells to G-quadruplex interactive compounds. *Nucleic Acids Res.*, **43**, 1759–1769.
- Ohnmacht,S.A. and Neidle,S. (2014) Small-molecule quadruplex-targeted drug discovery. *Bioorg. Med. Chem. Lett.*, **24**, 2602–2612.
- Lemarteleur,T., Gomez,D., Paterski,R., Mandine,E., Mailliet,P. and Riou,J.F. (2004) Stabilization of the c-myc gene promoter quadruplex by specific ligands' inhibitors of telomerase. *Biochem. Biophys. Res. Commun.*, **323**, 802–808.
- Leonetti,C., Scarsella,M., Riggio,G., Rizzo,A., Salvati,E., D'Incalci,M., Staszewsky,L., Frapolli,R., Stevens,M.F., Stoppacciaro,A. et al. (2008) G-quadruplex ligand RHPS4 potentiates the antitumor activity of camptothecins in preclinical models of solid tumors. *Clin. Cancer Res.*, **14**, 7284–7291.
- Biroccio,A., Porru,M., Rizzo,A., Salvati,E., D'Angelo,C., Orlandi,A., Passeri,D., Franceschin,M., Stevens,M.F., Gilson,E. et al. (2011) DNA damage persistence as determinant of tumor sensitivity to the combination of Topo I inhibitors and telomere-targeting agents. *Clin. Cancer Res.*, **17**, 2227–2236.
- Salvati,E., Scarsella,M., Porru,M., Rizzo,A., Iachettini,S., Tentori,L., Graziani,G., D'Incalci,M., Stevens,M.F., Orlandi,A. et al. (2010) PARP1 is activated at telomeres upon G4 stabilization: possible target for telomere-based therapy. *Oncogene*, **29**, 6280–6293.
- Lagah,S., Tan,I.L., Radhakrishnan,P., Hirst,R.A., Ward,J.H., O'Callaghan,C., Smith,S.J., Stevens,M.F., Grundy,R.G. and Rahman,R. (2014) RHPS4 G-quadruplex ligand induces anti-proliferative effects in brain tumor cells. *PLoS One*, **9**, e86187.
- Todaro,M., Alea,M.P., Di Stefano,A.B., Cammareri,P., Vermeulen,L., Iovino,F., Tripodo,C., Russo,A., Gulotta,G., Medema,J.P. et al. (2007) Colon cancer stem cells dictate tumor growth and resist cell death by production of interleukin-4. *Cell Stem Cell*, **1**, 389–402.
- Gowan,S.M., Heald,R., Stevens,M.F. and Kelland,L.R. (2001) Potent inhibition of telomerase by small-molecule pentacyclic acridines capable of interacting with G-quadruplexes. *Mol. Pharmacol.*, **60**, 981–988.

36. Biroccio,A., Benassi,B., Filomeni,G., Amodei,S., Marchini,S., Chiorino,G., Rotilio,G., Zupi,G. and Ciriolo,M.R. (2002) Glutathione influences c-Myc-induced apoptosis in M14 human melanoma cells. *J. Biol. Chem.*, **277**, 43763–43770.
37. Pagano,B., Amato,J., Iaccarino,N., Cingolani,C., Zizza,P., Biroccio,A., Novellino,O. and Randazzo,A. (2015) Looking for efficient G-quadruplex ligands: evidence for selective stabilizing properties and telomere damage by drug-like molecules. *ChemMedChem*, **10**, 640–649.
38. Cantor,C.R., Warshaw,M.M. and Shapiro,H. (1970) Oligonucleotide interactions. 3. Circular dichroism studies of the conformation of deoxyoligonucleotides. *Biopolymers*, **9**, 1059–1077.
39. Mergny,J.L., Li,J., Lacroix,L., Amrane,S. and Chaires,J.B. (2005) Thermal difference spectra: a specific signature for nucleic acid structures. *Nucleic Acids Res.*, **33**, e138.
40. Clevers,H. (2011) The cancer stem cell: premises, promises and challenges. *Nat med*, **17**, 313–319.
41. Bidzinska,J., Cimino-Reale,G., Zaffaroni,N. and Folini,M. (2013) G-quadruplex structures in the human genome as novel therapeutic targets. *Molecules*, **18**, 12368–12395.
42. Berardinelli,F., Siteni,S., Tanzarella,C., Stevens,M.F., Sgura,A. and Antoccia,A. (2015) The G-quadruplex-stabilising agent RHPS4 induces telomeric dysfunction and enhances radiosensitivity in glioblastoma cells. *DNA Rep. (Amst)*, **25**, 104–115.
43. Phatak,P., Cookson,J.C., Dai,F., Smith,V., Gartenhaus,R.B., Stevens,M.F. and Burger,A.M. (2007) Telomere uncapping by the G-quadruplex ligand RHPS4 inhibits clonogenic tumour cell growth in vitro and in vivo consistent with a cancer stem cell targeting mechanism. *Br. J. Cancer*, **96**, 1223–1233.
44. Leonetti,C., Amodei,S., D'Angelo,C., Rizzo,A., Benassi,B., Antonelli,A., Elli,R., Stevens,M.F., D'Incàlci,M., Zupi,G. et al. (2004) Biological activity of the G-quadruplex ligand RHPS4 (3,11-difluoro-6,8,13-trimethyl-8H-quino[4,3,2-k]acridinium methosulfate) is associated with telomere capping alteration. *Mol. Pharmacol.*, **66**, 1138–1146.
45. Rizzo,A., Salvati,E., Porru,M., D'Angelo,C., Stevens,M.F., D'Incàlci,M., Leonetti,C., Gilson,E., Zupi,G. and Biroccio,A. (2009) Stabilization of quadruplex DNA perturbs telomere replication leading to the activation of an ATR-dependent ATM signaling pathway. *Nucleic Acids Res.*, **37**, 5353–5364.
46. Iachettini,S., Stevens,M.F., Frigerio,M., Hummersone,M.G., Hutchinson,I., Garner,T.P., Searle,M.S., Wilson,D.W., Munde,M., Nanjunda,R. et al. (2013) On and off-target effects of telomere uncapping G-quadruplex selective ligands based on pentacyclic acridinium salts. *J. Exp. Clin. Cancer Res.*, **32**, 68–79.
47. Rizzo,A., Iachettini,S., Zizza,P., Cingolani,C., Porru,M., Artuso,S., Stevens,M., Hummersone,M., Biroccio,A., Salvati,E. et al. (2014) Identification of novel RHPS4-derivative ligands with improved toxicological profiles and telomere-targeting activities. *J. Exp. Clin. Cancer Res.*, **33**, 81–88.
48. Franceschin,M., Rizzo,A., Casagrande,V., Salvati,E., Alvino,A., Altieri,A., Ciammaichella,A., Iachettini,S., Leonetti,C., Ortagni,G. et al. (2012) Aromatic core extension in the series of N-cyclic bay-substituted perylene G-quadruplex ligands: increased telomere damage, antitumor activity, and strong selectivity for neoplastic over healthy cells. *ChemMedChem*, **7**, 2144–2154.
49. Porru,M., Artuso,S., Salvati,E., Bianco,A., Franceschin,M., Diodoro,M.G., Passeri,D., Orlandi,A., Savorani,F., D'Incàlci,M. et al. (2015) Targeting G-Quadruplex DNA Structures by Emicorin Has a Strong Antitumor Efficacy against Advanced Models of Human Colon Cancer. *Mol. Cancer Ther.*, **14**.
50. Reinhold,W.C., Mergny,J.L., Liu,H., Ryan,M., Pfister,T.D., Kinders,R., Parchment,R., Doroshow,J., Weinstein,J.N. and Pommier,Y. (2010) Exon array analyses across the NCI-60 reveal potential regulation of TOP1 by transcription pausing at guanosine quartets in the first intron. *Cancer Res.*, **70**, 2191–2203.
51. Kikin,O., D'Antonio,L. and Bagga,P.S. (2006) QGRS Mapper: a web-based server for predicting G-quadruplexes in nucleotide sequences. *Nucleic Acids Res.*, **34**, W676–W682.
52. Han,H., Hurley,L.H. and Salazar,M. (1999) A DNA polymerase stop assay for G-quadruplex-interactive compounds. *Nucleic Acids Res.*, **27**, 537–542.
53. Randazzo,A., Spada,G.P. and da Silva,M.W. (2013) Circular dichroism of quadruplex structures. *Top. Curr. Chem.*, **330**, 67–86.
54. Pagano,B., Cosconati,S., Gabelica,V., Petraccone,L., De Tito,S., Marinelli,L., La Pietra,V., di Leva,F.S., Lauri,I., Trotta,R. et al. (2012) State-of-the-art methodologies for the discovery and characterization of DNA G-quadruplex binders. *Curr. Pharm. Des.*, **18**, 1880–1899.
55. Guedin,A., Gros,J., Alberti,P. and Mergny,J.L. (2010) How long is too long? Effects of loop size on G-quadruplex stability. *Nucleic Acids Res.*, **38**, 7858–7868.
56. Piazza,A., Adrian,M., Samazan,F., Heddin,B., Hamon,F., Serero,A., Lopes,J., Teulade-Fichou,M.P., Phan,A.T. and Nicolas,A. (2015) Short loop length and high thermal stability determine genomic instability induced by G-quadruplex-forming minisatellites. *EMBO J.*, **34**, 1718–1734.
57. Hickson,I., Zhao,Y., Richardson,C.J., Green,S.J., Martin,N.M., Orr,A.I., Reaper,P.M., Jackson,S.P., Curtin,N.J. and Smith,G.C. (2004) Identification and characterization of a novel and specific inhibitor of the ataxia-telangiectasia mutated kinase ATM. *Cancer Res.*, **64**, 9152–9159.
58. Irollo,E. and Pirozzi,G. (2013) CD133: to be or not to be, is this the real question?. *Am. J. Transl. Res.*, **5**, 563–581.
59. Shmelkov,S.V., Butler,J.M., Hooper,A.T., Hormigo,A., Kushner,J., Milde,T., St Clair,R., Baljevic,M., White,I., Jin,D.K. et al. (2008) CD133 expression is not restricted to stem cells, and both CD133+ and CD133- metastatic colon cancer cells initiate tumors. *J. Clin. Invest.*, **118**, 2111–2120.
60. Elsaia,T.M., Martinez-Pomares,L., Robins,A.R., Crook,S., Seth,R., Jackson,D., McCart,A., Silver,A.R., Tomlinson,I.P. and Ilyas,M. (2010) The stem cell marker CD133 associates with enhanced colony formation and cell motility in colorectal cancer. *PLoS One*, **5**, e10714.
61. Li,Z. (2013) CD133: a stem cell biomarker and beyond. *Exp. Hematol. Oncol.*, **2**, 17–24.
62. Chambers,V.S., Marsico,G., Boutell,J.M., Di Antonio,M., Smith,G.P. and Balasubramanian,S. (2015) High-throughput sequencing of DNA G-quadruplex structures in the human genome. *Nat. Biotechnol.*, **33**, 877–881.
63. Rhodes,D. and Lipps,H.J. (2015) G-quadruplexes and their regulatory roles in biology. *Nucleic Acids Res.*, **43**, 8627–8637.
64. Huppert,J.L. and Balasubramanian,S. (2005) Prevalence of quadruplexes in the human genome. *Nucleic Acids Res.*, **33**, 2908–2916.
65. Gomez,D., Guedin,A., Mergny,J.L., Salles,B., Riou,J.F., Teulade-Fichou,M.P. and Calsou,P. (2010) A G-quadruplex structure within the 5'-UTR of TRF2 mRNA represses translation in human cells. *Nucleic Acids Res.*, **38**, 7187–7198.
66. Maizels,N. (2012) G4 motifs in human genes. *Ann. N. Y. Acad. Sci.*, **1267**, 53–60.
67. Fargeas,C.A., Huttner,W.B. and Corbeil,D. (2007) Nomenclature of prominin-1 (CD133) splice variants - an update. *Tissue Antigens*, **69**, 602–606.
68. Kemper,K., Sprick,M.R., de Bree,M., Scopelliti,A., Vermeulen,L., Hoek,M., Zeilstra,J., Pals,S.T., Mehmet,H., Stassi,G. et al. (2010) The AC133 epitope, but not the CD133 protein, is lost upon cancer stem cell differentiation. *Cancer Res.*, **70**, 719–729.
69. Mak,A.B., Nixon,A.M., Kittanakom,S., Stewart,J.M., Chen,G.I., Curak,J., Gingras,A.C., Mazitschek,R., Neel,B.G., Stagliar,I. et al. (2012) Regulation of CD133 by HDAC6 promotes beta-catenin signaling to suppress cancer cell differentiation. *Cell Rep.*, **2**, 951–963.
70. Shimozato,O., Waraya,M., Nakashima,K., Souda,H., Takiguchi,N., Yamamoto,H., Takenobu,H., Uehara,H., Ikeda,E., Matsushita,S. et al. (2015) Receptor-type protein tyrosine phosphatase kappa directly dephosphorylates CD133 and regulates downstream AKT activation. *Oncogene*, **34**, 1949–1960.